

Pseudocodeword-based Decoding of Quantum Stabilizer Codes

July X. Li and Pascal O. Vontobel

Department of Information Engineering, The Chinese University of Hong Kong, Hong Kong

Email: {july.x.li, pascal.vontobel}@ieee.org

Abstract—It has been shown that graph-cover pseudocodewords can be used to characterize the behavior of sum-product algorithm (SPA) decoding of classical codes. In this paper, we leverage and adapt these results to analyze SPA decoding of quantum stabilizer codes. We use the obtained insights to formulate modifications to the SPA that overcome some of its weaknesses.

I. INTRODUCTION

Graph covers have been shown to be a useful tool for analyzing sum-product algorithm (SPA) decoding of classical codes [1]. The task of analyzing the behavior of SPA decoding for quantum stabilizer codes is more challenging, especially because the degeneracy of quantum stabilizer codes needs to be taken into account. Despite these challenges, being able to understand and improve the behavior of the SPA is highly desirable, since it has been observed that the performance of the SPA is far from satisfactory when decoding quantum stabilizer codes of high degeneracy (see, e.g., the discussion of simulation results of various message-passing iterative decoding algorithms and LP decoders in [2]–[4]).

In this paper, in a first step, we use graph-cover pseudocodewords to analyze the behavior of SPA. In particular, we can show that the decoding ability of the SPA is limited by the minimum distance of the normalizer label code, which is a serious problem for quantum LDPC codes, e.g., the toric codes [5] and MacKay’s bicycle codes [6], where the minimum distance of the normalizer label code is no larger than the row weight of its parity-check matrix due to the self-orthogonality of the stabilizer label code.

In a second step, we use the obtained insights to formulate modifications to the SPA that overcome some of its weaknesses. Taking advantage of the degeneracy of the quantum stabilizer code, the performance of the decoder is then limited by the minimum distance of the quantum stabilizer code d instead of the minimum distance of the normalizer label code $d_{\mathcal{N}}$. For notational details, see Section II-A.

This paper is organized as follows. In Section II, we review some basic notations including the stabilizer formalism and the standard SPA for quantum stabilizer codes. In Section III, we analyze the performance of SPA for quantum stabilizer codes and give some other theoretical results about degenerate decoders of quantum stabilizer codes. In Section IV, we propose, first, some methods to improve the performance of the SPA for general quantum stabilizer codes and, second,

a pseudocodeword-based decoder for quantum cycle codes. Finally, we show some simulation results in Section V.

II. BASICS

A. Quantum Stabilizer Formalism

We refer the readers to [7], [8] for a detailed introduction to quantum stabilizer codes, some recent developments of quantum error-correction codes, and more details of the notations. Moreover, see [3] for the use of pseudocodewords in the context of quantum stabilizer codes. Due to the page limitations, we only introduce the essential notations which are used throughout the paper.

Consider an $[[n, k, d]]$ quantum stabilizer code \mathcal{C} of length n , dimension k , and minimum distance d . The quantum stabilizer code \mathcal{C} may be characterized using the equivalent binary representation of its stabilizer, namely its binary stabilizer label code \mathcal{B} , which is self-orthogonal under the symplectic inner product to guarantee the commutativity of the generators of the stabilizer. The binary representation of a Pauli operator on n qubits is a length- $2n$ binary vector $\mathbf{v} = [\mathbf{v}_1, \dots, \mathbf{v}_n] \in (\mathbb{F}_2^2)^n$, where each \mathbf{v}_i is obtained by mapping I, X, Y , and Z onto \mathbb{F}_2^2 as follows

$$I \mapsto [0, 0], \quad X \mapsto [1, 0], \quad Y \mapsto [1, 1], \quad \text{and} \quad Z \mapsto [0, 1],$$

and the weights of them are defined to be, respectively,

$$\text{wt}([0, 0]) \triangleq 0 \quad \text{and} \quad \text{wt}([1, 0]) = \text{wt}([1, 1]) = \text{wt}([0, 1]) \triangleq 1.$$

In this paper, we make the following assumptions:

- the normalizer label code \mathcal{N} is the dual code of \mathcal{B} under the symplectic inner product (note that the self-orthogonality of \mathcal{B} implies that $\mathcal{B} \subseteq \mathcal{N}$);
- both \mathcal{B} and \mathcal{N} are binary linear codes of length $2n$ and of dimension $n - k$ and $n + k$, respectively;
- the weight of \mathbf{v} is $\text{wt}(\mathbf{v}) \triangleq \sum_i \text{wt}(\mathbf{v}_i)$;
- $d \triangleq \min_{\mathbf{v} \in \mathcal{N} \setminus \mathcal{B}} \text{wt}(\mathbf{v})$ and $t \triangleq \lfloor \frac{d-1}{2} \rfloor$;
- $d_{\mathcal{N}} \triangleq \min_{\mathbf{v} \in \mathcal{N}} \text{wt}(\mathbf{v})$ and $t_{\mathcal{N}} \triangleq \lfloor \frac{d_{\mathcal{N}}-1}{2} \rfloor$.

A quantum stabilizer code \mathcal{C} is called a quantum cycle code if its normalizer label code \mathcal{N} is a cycle code, which means that the number of 1’s per column of the parity-check matrix H describing \mathcal{N} is two. For example, the toric codes are quantum cycle codes (see, e.g., [5], [9]).

The quantum channel that we use in this paper is the quantum depolarizing channel (QDCh). Similar to the binary symmetric channel (BSC), the action of a QDCh with depolarizing probability p is such that it acts independently on each

qubit: a qubit is either unchanged with probability $1-p$, or affected by a unitary operator X , Y , or Z , each with probability $p/3$. Since we are decoding with respect to *binary* normalizer label codes, decoding is based on approximating the QDCh by two independent BSCs with crossover probability $2p/3$, i.e., the probability for having a bit-flip and a phase-flip is $2p/3$ independently for each qubit.

Definition 1. Given a syndrome $\mathbf{s} \in \mathbb{F}_2^{n-k}$, let $\mathbf{s} \mapsto \mathbf{t}(\mathbf{s})$ be the mapping giving a coset representative of the coset of \mathcal{N} corresponding to the syndrome \mathbf{s} . Note that if \mathbf{e} is the binary representation of the actual error, then $H\mathbf{e}^\top = \mathbf{s}^\top$ and $\mathbf{e} \in \mathbf{t}(\mathbf{s}) + \mathcal{N}$.

A non-degenerate decoder \mathcal{D}_{ND} outputs a vector based on the syndrome \mathbf{s} ; an error vector \mathbf{v} leads to a decoding error for \mathcal{D}_{ND} if $\mathbf{v} \neq \mathcal{D}_{\text{ND}}(\mathbf{v}H^\top)$. A degenerate decoder \mathcal{D}_{D} outputs a coset of \mathcal{B} based on the syndrome \mathbf{s} ; an error vector \mathbf{v} leads to a decoding error for \mathcal{D}_{D} if $\mathbf{v} \notin \mathcal{D}_{\text{D}}(\mathbf{v}H^\top)$. The blockwise ML (non-)degenerate decoders $\mathcal{D}_{\text{ND}}^{\text{ML}}$, $\mathcal{D}_{\text{D}}^{\text{ML}*}$, and $\mathcal{D}_{\text{D}}^{\text{ML}}$ are defined to be, respectively,

$$\mathcal{D}_{\text{ND}}^{\text{ML}}(\mathbf{s}) \triangleq \arg \min_{\mathbf{v} \in \mathbf{t}(\mathbf{s}) + \mathcal{N}} \text{wt}(\mathbf{v}), \quad \mathcal{D}_{\text{D}}^{\text{ML}*}(\mathbf{s}) \triangleq \mathcal{D}_{\text{ND}}^{\text{ML}}(\mathbf{s}) + \mathcal{B},$$

$$\mathcal{D}_{\text{D}}^{\text{ML}}(\mathbf{s}) \triangleq \arg \max_{\ell + \mathcal{B}: \ell \in \mathbf{t}(\mathbf{s}) + \mathcal{N}} p(\ell + \mathcal{B} | \mathbf{s}),$$

where $p(\ell + \mathcal{B} | \mathbf{s})$ is the probability of the coset $\ell + \mathcal{B}$ based on the syndrome \mathbf{s} . ■

For the simulations in this paper, there is a decoding error if the output vector is not in the same coset of \mathcal{B} as the actual error or the output coset is not the same coset of \mathcal{B} as the coset of the actual error.

B. SPA decoding, graph covers, and pseudocodewords

SPA decoding of a quantum stabilizer code \mathcal{C} consists of the following steps: 1) running the SPA on a factor graph representing a coset of the normalizer label code \mathcal{N} , where the coset is defined by the syndrome \mathbf{s} that is obtained from suitable quantum measurements; 2) outputting a vector \mathbf{v} , 3) finding the coset of \mathcal{B} containing \mathbf{v} . (For further details, see, e.g., [2, Section IV].) In this paper, the factor graphs are normal factor graphs, where variables are associated with edges.

It was shown in [10] that fixed points of the SPA correspond to stationary points of the Bethe free energy function. As discussed in [1], for LDPC codes this means that the beliefs obtained at a fixed point of the SPA induce a pseudocodeword ω . For example, if we consider a binary linear code, then the i^{th} component of ω is $\omega_i \triangleq b_i(1)$ assuming the belief of the i^{th} variable is $[b_i(0), b_i(1)]$. The paper [1] also introduced the symbolwise graph-cover decoder, a decoder that finds the pseudocodeword with minimal Bethe free energy, or, equivalently, the pseudocodeword with the most pre-images in all M -covers of the base normal factor graph (after properly discounting for a channel-output-dependent term), when M goes to infinity. For general codes, symbolwise graph-cover decoding is an approximation of the true behavior of SPA

decoding. However, for cycle codes it was shown in [11] that SPA decoding is equivalent to symbolwise graph-cover decoding. Note that, although symbolwise graph-cover decoding is based on M -covers where M goes to infinity, in many instances the study of pseudocodewords induced by codewords in M -covers for small M gives already many insights into the suboptimality of SPA decoding (see, e.g., the upcoming Fig. 2 that shows an M -cover for $M = 2$).

III. THEORETICAL ANALYSIS

In this section we characterize the performance of the non-degenerate and degenerate decoders defined in Definition 1. In particular, in Theorems 2 and 3 we prove that the minimum weight of errors that the non-degenerate and degenerate decoders fail to decode are $t_{\mathcal{N}} + 1$ and $t + 1$, respectively. Moreover, in Theorems 4 and 5, we show two types of decoding errors limiting the performance of SPA decoding of quantum cycle codes.

Theorem 2. *The minimum weight of errors leading to decoding errors for $\mathcal{D}_{\text{ND}}^{\text{ML}}$ is $t_{\mathcal{N}} + 1$.*

Proof. See Appendix A. □

Theorem 3. *The minimum weights of errors leading to decoding errors for $\mathcal{D}_{\text{D}}^{\text{ML}}$ and $\mathcal{D}_{\text{D}}^{\text{ML}*}$ both are $t + 1$.*

Proof. See Appendix B. □

Theorem 4. *The minimum weight of errors that the SPA fails to decode for a toric code is 2. For a $[[2L^2, 2, L]]$ toric code with $L \geq 5$, the number of such weight-2 errors is $12L^2$.*

Proof. For a $[[2L^2, 2, L]]$ toric code \mathcal{C} with $L < 5$, it cannot correct some weight-2 errors because of its minimum distance. For a $[[2L^2, 2, L]]$ toric code \mathcal{C} with $L \geq 5$, there are two types of weight-2 errors that cannot be corrected using SPA decoding as shown in Fig. 1. (Here and for other similar figures we use the drawing conventions listed in Table I; moreover, edges with components close to 0 are not drawn). For both cases, we obtain an SPA pseudocodeword $\omega = [\omega, \omega, \omega, \omega]$, for some $\omega \in (0, 1]$. When the SPA decoder makes hard decisions based on ω , it outputs either $[0, 0, 0, 0]$ or $[1, 1, 1, 1]$ and hence fails to match the syndrome. The minimum weight of errors resulting in decoding failures for toric codes is 2, since weight-1 errors can be corrected. If we count the number of such weight-2 errors, there are 6 in each length-4 cycle and $12L^2$ in total. □

For a quantum cycle code with even $d_{\mathcal{N}}$, the minimum weight of errors that the SPA fails to decode is no larger than $d_{\mathcal{N}}/2$ because of similar problems as in Fig. 1.

Theorem 5. *The minimum weight of errors that the SPA fails to decode for a toric code is no larger than $d_{\mathcal{N}}$.*

Proof. We want to show that there exist errors of weight $d_{\mathcal{N}}$ that the SPA fails to decode. Since the minimum weight of vectors in the normalizer label code \mathcal{N} is $d_{\mathcal{N}}$, there exists a cycle of length $d_{\mathcal{N}}$ in \mathcal{N} and we assume that the error is a path of length $d_{\mathcal{N}}$ starting from any check involved

TABLE I: Drawing conventions for figures.

empty vertex	$s_i = 0$ for syndrome bit associated with i -th parity check
filled vertex	$s_i = 1$ for syndrome bit associated with i -th parity check
black edge	channel introduced no error at that location
red edge	channel introduced an error at that location

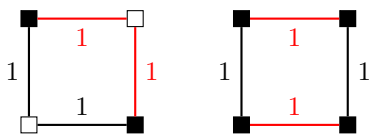


Fig. 1: Rescaled pseudocodewords of a toric code.

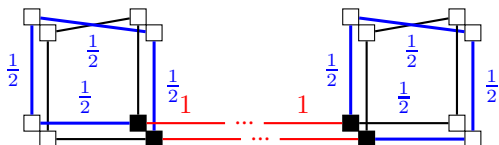


Fig. 2: Pseudocodewords (blue or red) of a toric code.

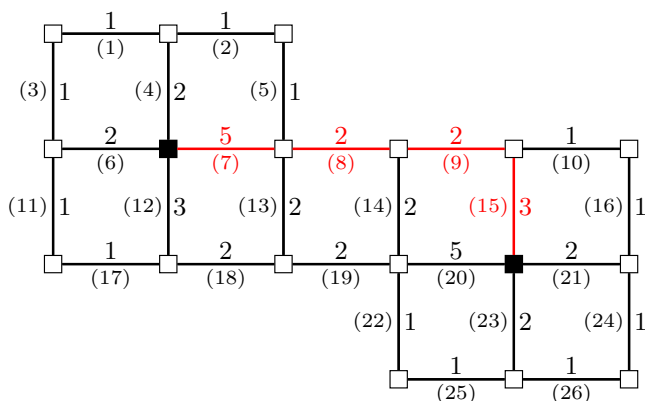


Fig. 3: A rescaled pseudocodeword of a toric code, where component $\tilde{\omega}_i$ and index (i) are shown next to the i^{th} edge.

in that cycle. Fig. 2 is a 2-cover of the relevant part of a toric code. We claim that the SPA cannot decode the above-mentioned error. The reason is as follows. There are two valid configurations in the 2-cover, where the red one can be projected down as a codeword with a valid syndrome, while the blue one cannot. The components of the pseudocodewords resulting from these valid configurations are shown next to the corresponding edges in Fig. 2. The SPA pseudocodeword is a linear combination of such pseudocodewords, e.g., a rescaled SPA pseudocodeword in Fig. 3, and the SPA decoder fails to output a vector with a valid syndrome no matter how to scale such SPA pseudocodeword. \square

More generally, for quantum cycle codes, the SPA fails to decode errors of minimum weight no larger than $d_{\mathcal{N}}/2$ for similar reasons.

IV. PSEUDOCODEWORD-BASED DECODING

If we want to improve the performance of SPA of quantum stabilizer cycle codes, or, more generally, quantum stabilizer codes, the first task is to address the problem mentioned in the proof of Theorem 4 by breaking the symmetry of the SPA to avoid ending up with pseudocodewords like the ones in Fig. 1.

A. Reweighted SPA Decoding

Our first approach is to use the reweighted SPA decoding proposed in [12], which reweights message calculations. However, instead of uniformly reweighting the messages, we randomly select weights from a certain interval. We call the resulting algorithm randomly reweighted SPA (RR-SPA). Empirically, this method can improve the performance of SPA decoding of the toric codes, but there is not much improvement for MacKay’s bicycle codes.

B. Initial-message-reweighted SPA of Quantum Stabilizer Codes

In order to introduce our second approach, we recall that the SPA is based on the log-likelihood ratios (LLRs) $\gamma_i \triangleq \log\left(\frac{\Pr(E_i=0)}{\Pr(E_i=1)}\right)$ and the syndrome \mathbf{s} . Our second approach is called initial-message-reweighted SPA (IMR-SPA) and described in Algorithm 1. The IMR-SPA also runs the SPA, however, with the reweighted LLRs, i.e., γ_i is replaced by $\alpha_i \gamma_i$, where α_i is a weighting factor randomly generated from some interval. Empirically, it is observed that the RR-SPA and the IMR-SPA have similar performance for the toric codes. From an analysis point of view, the IMR-SPA may be preferable compared to the RR-SPA and other approaches like random perturbation [13], because after suitable adaptations, we can apply the Bethe free energy framework [1], [10], [11] to analyze the IMR-SPA.

We briefly explain why the IMR-SPA helps to improve the performance of SPA decoding of quantum stabilizer codes. Namely, assume that we know, for analysis purposes, the actual error vector $\tilde{\mathbf{e}}$. For SPA decoding, using the LLR vector γ with the syndrome \mathbf{s} is equivalent to using the LLR vector $\tilde{\gamma}$, where $\tilde{\gamma}_i \triangleq (-1)^{\tilde{e}_i} \gamma_i$, with the syndrome $\mathbf{0}$. SPA decoding succeeds when it converges to the all-zero vector based on the LLR vector $\tilde{\gamma}$ and the syndrome $\mathbf{0}$. The IMR-SPA changes the LLR vector for the standard SPA from $\tilde{\gamma}_i$ to be $\alpha_i \tilde{\gamma}_i$ and hence may move some $\tilde{\gamma}$ from the “bad” region to the “good” region in which the SPA converges to the all-zero vector.

C. Pseudocodeword-based Decoder of Quantum Cycle Codes

For quantum cycle codes, the IMR-SPA decoding can improve the minimum weight of errors leading to decoding failures beyond $d_{\mathcal{N}}/2$, but it is still limited by the problems mentioned in Theorem 5. Therefore, we propose a pseudocodeword-based decoder abbreviated as SPA-PCWD, which is described in Algorithm 2, to further improve the performance of SPA decoding for quantum cycle codes. When SPA decoding fails to output a vector with valid syndrome, we hope to make use of the SPA pseudocodeword to obtain one with valid syndrome. There are two difficulties in this

Algorithm 1 Initial-message-reweighted SPA (IMR-SPA)

Input: the syndrome \mathbf{s} , the maximum number of SPA iterations, and the reweighting range $[a, b]$.

Output: $\mathbf{v} + \mathcal{B}$.

- 1: Use SPA to obtain an output vector \mathbf{v} .
 - 2: **if** $H\mathbf{v}^\top = \mathbf{s}^\top$ (equivalently $\mathbf{v} \in \mathbf{t}(\mathbf{s}) + \mathcal{N}$) **then**
 - 3: Output $\mathbf{v} + \mathcal{B}$.
 - 4: **else**
 - 5: **while** $H\mathbf{v}^\top \neq \mathbf{s}^\top$ **do**
 - 6: For the i^{th} variable, randomly generate a weighting factor $\alpha_i \in [a, b]$ and reweight the LLR to the SPA from γ_i to be $\alpha_i\gamma_i$.
 - 7: Use SPA to obtain an output vector \mathbf{v} .
 {Set the max. number of trial times if necessary.}
 - 8: **end while**
 - 9: Output $\mathbf{v} + \mathcal{B}$.
 - 10: **end if**
-

task: 1) the components contributed by codewords from graph covers without a valid syndrome need to be removed; 2) the components contributed by codewords from graph covers with a valid syndrome are mixed together and need to be separated.

The main idea of the decoder is to first decompose the pseudocodeword ω into a set of paths and then output a vector \mathbf{v} with a valid syndrome, where the support of \mathbf{v} is determined by a collection of paths. The paths are obtained by starting from an unsatisfied check s_i and by always following the edge with the largest possible component of ω for the next step without repetition until reaching an unsatisfied check $s_{i'}$, where the weight of the path is defined as the minimum component of ω on that path. The contribution of that path from the pseudocodeword is then subtracted and the path is included in the set of candidate paths. We use a simple example to explain the procedure of Algorithm 2.

Example 6. Consider a $\llbracket 2L^2, 2, L \rrbracket$ toric code of $L = 9$ and $p = 0.0123$. We obtain an SPA pseudocodeword ω after 100 iterations. The rescaled pseudocodeword $\tilde{\omega} \triangleq \omega/0.0836$ is shown in Fig. 3, where edges with component $\tilde{\omega}_i < 0.005$ are omitted. First, by Algorithm 3 we can obtain a set of paths P , e.g., $P_1 = \{7, 8, 9, 15\}$ and $P_2 = \{7, 13, 19, 20\}$ with $\hat{\omega}_i = 2$ and $S_i = \{1, 2\}$ for $i = 1, 2$. Then, Algorithm 2 picks an arbitrary path P_{i^*} since their costs are the same and outputs $\mathbf{v} + \mathcal{B}$, where the support of \mathbf{v} is determined by P_{i^*} .

V. SIMULATION RESULTS

Fig. 4 shows some simulation results of SPA+LPPCWD decoding of toric codes described in Algorithm 2, where we use at most 100 iterations of SPA to obtain SPA pseudocodewords. According to the simulation results in [4], the performance of the original SPA gets worse as the code block length of toric codes increases. As shown in Fig. 4, the performance of the SPA+LPPCWD improves as the code block length of toric codes increases and the SPA+LPPCWD has similar performance as the neural belief-propagation decoder

Algorithm 2 Pseudocodeword-based decoder (SPA+PCWD) for quantum cycle codes

Input: the syndrome \mathbf{s} and the max. number of SPA iterations.

Output: $\mathbf{v} + \mathcal{B}$.

- 1: Use SPA to find an output vector \mathbf{v} and obtain an SPA pseudocodeword ω .
 - 2: **if** $H\mathbf{v}^\top = \mathbf{s}^\top$ **then**
 - 3: Return $\mathbf{v} + \mathcal{B}$.
 - 4: **else**
 - 5: Obtain $P = \{P_i\}$, $\{S_i\}$, and $\hat{\omega}$ by Algorithm 3.
 - 6: $\mathbf{v} \leftarrow \mathbf{0}$.
 - 7: $\mathcal{J} \leftarrow \{j \mid s_j \neq 0\}$ {The index set of unsatisfied checks.}
 - 8: **while** $\mathcal{J} \neq \emptyset$ and $P \neq \emptyset$ **do**
 - 9: $i \leftarrow \arg \min_{j: P_j \in P} (1 - \hat{\omega}_j) \cdot |P_j|$. {Minimize cost.}
 - 10: $v_j \leftarrow 1 \forall j \in P_i$. {Update \mathbf{v} w.r.t. P_i .}
 - 11: $\mathcal{J} \leftarrow \mathcal{J} \setminus S_i$. {Update unsatisfied checks.}
 - 12: $P \leftarrow \{P_j \in P \mid S_j \subseteq \mathcal{J}, P_j \subseteq \{\ell \mid v_\ell = 0\}\}$.
 {Update the set of available paths.}
 - 13: **end while**
 {A modification of this algorithm with the above while loop replaced by an LP with cost for each path P_i as $\lambda_i \triangleq (1 - \hat{\omega}_i) \cdot |P_i|$ is referred as SPA+LPPCWD.}
 - 14: **end if**
-

Algorithm 3 Pseudocodeword decomposition (PCWD) for quantum cycle codes

Input: a pseudocodeword ω and the syndrome \mathbf{s} .

Output: A set of paths $P = \{P_i\}$, a set of corresponding end checks $S = \{S_i\}$, and a weight vector $\hat{\omega}$.

- 1: $\mathcal{J} \leftarrow \{j \mid s_j \neq 0\}$, $P \leftarrow \emptyset$, and $S \leftarrow \emptyset$.
 - 2: **while** $\mathcal{J} \neq \emptyset$ **do**
 - 3: Start from each s_j , $j \in \mathcal{J}$, and follow the edge with the largest possible component of ω at each step without repetition until reaching $s_{j'}$, $j' \in \mathcal{J}$, to obtain a path P_j with weight $\bar{\omega}_j \leftarrow \min_{\ell \in P_j} \omega_\ell$ and $S_j \leftarrow \{j, j'\}$.
 - 4: $i \leftarrow \arg \min_{j: P_j \in P} (1 - \bar{\omega}_j) \cdot |P_j|$. {Find min. cost one.}
 - 5: $\omega_\ell \leftarrow \omega_\ell - \bar{\omega}_i \forall \ell \in P_i$. {Subtract P_i 's contribution.}
 - 6: $P \leftarrow P \cup \{P_i\}$, $S \leftarrow S \cup \{S_i\}$, and $\hat{\omega}_i \leftarrow \bar{\omega}_i$ if $i \neq i'$.
 {Include P_i in P if P_i is a path.}
 - 7: $\mathcal{J} \leftarrow \mathcal{J} \setminus \{j \in \mathcal{J} \mid \bar{\omega}_j = 0\}$. {Remove isolated checks.}
 - 8: **end while**
-

in [4] and the Markov chain Monte Carlo algorithm in [14]. Fig. 5 shows the weight distribution of the decoding errors of SPA+PCWD decoding of toric codes, where the minimum weight of errors increases as the block length increases. We also observed that the IMR-SPA and the RR-SPA have similar performance as the SPA+PCWD for toric codes with $L < 9$, but unfortunately they are limited by some weight-4 errors for $L \geq 9$.

Fig. 6 shows some simulation results of the IMR-SPA of a $\llbracket 256, 32 \rrbracket$ MacKay's bicycle code with the total row weight

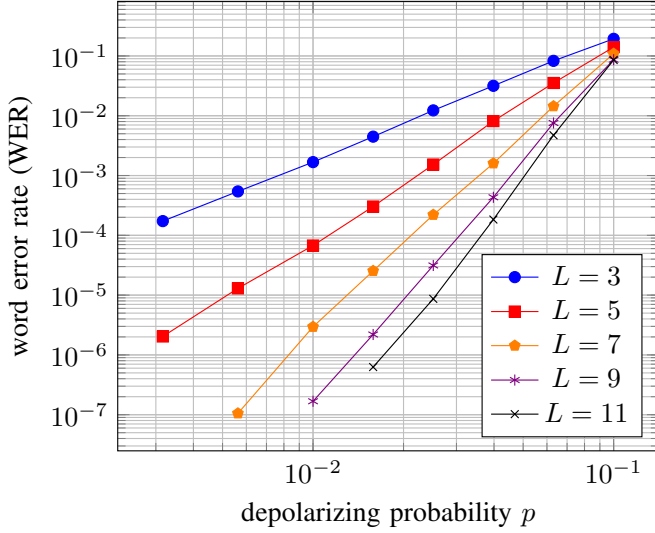


Fig. 4: Simulation results of SPA+LPPCWD for toric codes.

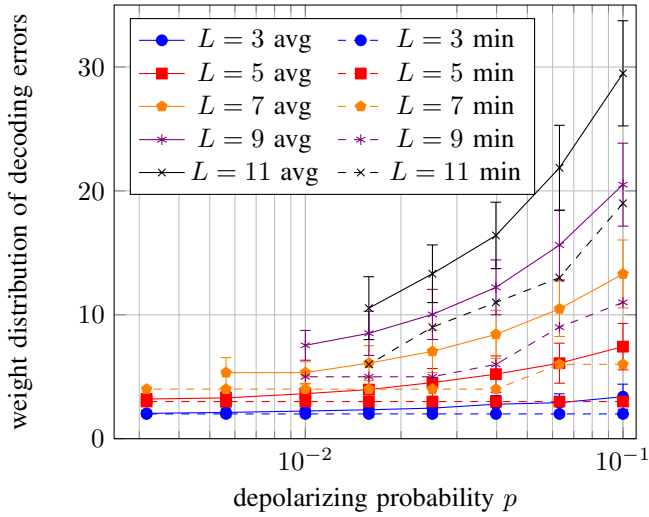


Fig. 5: Weight distribution of decoding errors of SPA+PCWD for toric codes (solid: average, dashed: minimum).

16 for \mathcal{N} . The maximum number of iterations of SPA is 100 and the maximum number of IMR trials is 10. The IMR-SPA achieves lower WER at around $p = 10^{-2}$ compared with the the neural belief-propagation decoder [4] for MacKay's bicycle codes with the same parameters.

APPENDIX A PROOF OF THEOREM 2

Proof sketch: The idea is to show each coset of \mathcal{N} contains at most one vector of weight less than or equal to $t_{\mathcal{N}}$ and there exists some coset of \mathcal{N} containing two vectors of weights less than or equal to $t_{\mathcal{N}} + 1$, one of which is a decoding error.

Let the set of decoding errors and the minimum weight of decoding errors for \mathcal{D}_A^B be $\mathcal{E}_A^B \triangleq \mathbb{F}_2^{2n} \setminus (\cup_s \mathcal{D}_A^B(s))$ and

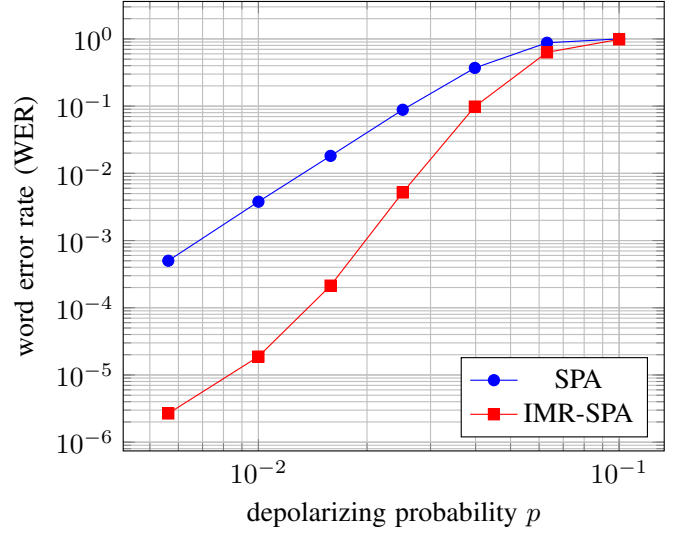


Fig. 6: Simulation results for SPA and IMR-SPA decoding of a $[[256, 32]]$ MacKay's bicycle code.

$d_A^B \triangleq \min_{\mathbf{v} \in \mathcal{E}_A^B} \text{wt}(\mathbf{v})$. We show that $d_{\text{ND}}^{\text{ML}} \geq t_{\mathcal{N}} + 1$ and $d_{\text{ND}}^{\text{ML}} \leq t_{\mathcal{N}} + 1$.

- ($d_{\text{ND}}^{\text{ML}} \geq t_{\mathcal{N}} + 1$) For any syndrome $\mathbf{s} \in \mathbb{F}_2^{n-k}$, there is at most one $\mathbf{v} \in \mathbf{t}(\mathbf{s}) + \mathcal{N}$ such that $\text{wt}(\mathbf{v}) \leq t_{\mathcal{N}}$, otherwise suppose there are $\mathbf{v}_1, \mathbf{v}_2 \in \mathbf{t}(\mathbf{s}) + \mathcal{N}$ such that $\text{wt}(\mathbf{v}_1), \text{wt}(\mathbf{v}_2) \leq t_{\mathcal{N}}$ and then $\mathbf{v}_1 + \mathbf{v}_2 \in \mathcal{N}$ with $\text{wt}(\mathbf{v}_1 + \mathbf{v}_2) \leq 2t_{\mathcal{N}} < d_{\mathcal{N}}$. A contradiction arises. Hence for all the vectors with weight no more than $t_{\mathcal{N}}$, they must have distinct syndromes and they are all in $\cup_s \mathcal{D}_{\text{ND}}^{\text{ML}}(\mathbf{s})$ and not in $\mathcal{E}_{\text{ND}}^{\text{ML}}$, which implies $d_{\text{ND}}^{\text{ML}} \geq t_{\mathcal{N}} + 1$.
- ($d_{\text{ND}}^{\text{ML}} \leq t_{\mathcal{N}} + 1$) Since $d_{\mathcal{N}} = \min_{\mathbf{v} \in \mathcal{N}} \text{wt}(\mathbf{v})$, there exists $\mathbf{v} \in \mathcal{N}$ such that $\text{wt}(\mathbf{v}) = d_{\mathcal{N}}$. There exist $\mathbf{v}_1, \mathbf{v}_2 \in \mathbb{F}_2^{2n}$ such that $\mathbf{v}_1 + \mathbf{v}_2 = \mathbf{v}$, $\text{wt}(\mathbf{v}_2) = t_{\mathcal{N}} + 1$, and $\text{wt}(\mathbf{v}_1) = d_{\mathcal{N}} - \text{wt}(\mathbf{v}_2) \leq d_{\mathcal{N}} - (t_{\mathcal{N}} + 1) \leq t_{\mathcal{N}} + 1$. Then $\mathbf{v}_1, \mathbf{v}_2 \in \mathbf{t}(\mathbf{s}) + \mathcal{N}$ for some \mathbf{s} and at most one of them can be in $\mathcal{D}_{\text{ND}}^{\text{ML}}(\mathbf{s})$. Hence $\mathbf{v}_i \in \mathcal{E}_{\text{ND}}^{\text{ML}}$ for some i and $d_{\text{ND}}^{\text{ML}} \leq \text{wt}(\mathbf{v}_i) \leq t_{\mathcal{N}} + 1$.

APPENDIX B PROOF OF THEOREM 3

Let the set of decoding errors and the minimum weight of decoding errors for \mathcal{D}_A^B be $\mathcal{E}_A^B \triangleq \mathbb{F}_2^{2n} \setminus (\cup_s \mathcal{D}_A^B(s))$ and $d_A^B \triangleq \min_{\mathbf{v} \in \mathcal{E}_A^B} \text{wt}(\mathbf{v})$. We first show that $d_D^{\text{ML}*}, d_D^{\text{ML}} \leq t + 1$ and then $d_D^{\text{ML}*} \geq t + 1$.

- ($d_D^{\text{ML}*}, d_D^{\text{ML}} \leq t + 1$) Since $d \triangleq \min_{\mathbf{v} \in \mathcal{N} \setminus \mathcal{B}} \text{wt}(\mathbf{v})$, there exists $\mathbf{v} \in \mathcal{N} \setminus \mathcal{B}$ such that $\text{wt}(\mathbf{v}) = d$. There exist $\mathbf{v}_1, \mathbf{v}_2 \in \mathbb{F}_2^{2n}$ such that $\mathbf{v}_1 + \mathbf{v}_2 = \mathbf{v}$, $\text{wt}(\mathbf{v}_2) = t + 1$, and $\text{wt}(\mathbf{v}_1) = d - \text{wt}(\mathbf{v}_2) \leq d_{\mathcal{N}} - (t + 1) \leq t + 1$. Then we have $\mathbf{v}_1 \in \mathbf{t}(\mathbf{s}) + \ell_1 + \mathcal{B}$ and $\mathbf{v}_2 \in \mathbf{t}(\mathbf{s}) + \ell_2 + \mathcal{B}$, for some \mathbf{s} and $\ell_1 \neq \ell_2 \in \mathcal{N}$. Then at most one of them can be in $\mathcal{D}_D^{\text{ML}*}(\mathbf{s})$ or $\mathcal{D}_D^{\text{ML}}(\mathbf{s})$. Hence $\mathbf{v}_{i_1} \in \mathcal{E}_D^{\text{ML}*}$ and $\mathbf{v}_{i_2} \in \mathcal{E}_D^{\text{ML}}$ for some i_1, i_2 and $d_D^{\text{ML}*} \leq \text{wt}(\mathbf{v}_{i_1}) \leq t_{\mathcal{N}} + 1$ and $d_D^{\text{ML}} \leq \text{wt}(\mathbf{v}_{i_2}) \leq t_{\mathcal{N}} + 1$.

- ($d_D^{\text{ML}^*} \geq t + 1$) For any syndrome $\mathbf{s} \in \mathbb{F}_2^{n-k}$, there is at most one coset of \mathcal{B} in $\mathbf{t}(\mathbf{s}) + \mathcal{N}$ containing vectors of weights smaller or equal to t , otherwise suppose there are $\mathbf{v}_1, \mathbf{v}_2 \in \mathbf{t}(\mathbf{s}) + \mathcal{N}$ with $\text{wt}(\mathbf{v}_1), \text{wt}(\mathbf{v}_2) \leq t$ such that $\mathbf{v}_1 \in \mathbf{t}(\mathbf{s}) + \ell_1 + \mathcal{B}$ and $\mathbf{v}_2 \in \mathbf{t}(\mathbf{s}) + \ell_2 + \mathcal{B}$ for $\ell_1 \neq \ell_2 \in \mathcal{N}$, and then $\mathbf{v}_1 + \mathbf{v}_2 \in \mathcal{N} \setminus \mathcal{B}$ with $\text{wt}(\mathbf{v}_1 + \mathbf{v}_2) \leq 2t < d$. A contradiction arises. Hence all vectors of weight no larger than t are in $\cup_{\mathbf{s}} \mathcal{D}_D^{\text{ML}^*}(\mathbf{s})$ and not in $\mathcal{E}_D^{\text{ML}}$, which implies $d_D^{\text{ML}^*} \geq t + 1$.

The main contribution of the probabilities of cosets comes from the vectors with minimum weights as $p \rightarrow 0$. Hence $d_D^{\text{ML}} \geq d_D^{\text{ML}^*} \geq t + 1$ which implies $d_D^{\text{ML}} = t + 1$.

REFERENCES

- [1] P. O. Vontobel, "Counting in graph covers: A combinatorial characterization of the Bethe entropy function," *IEEE Trans. Inf. Theory*, vol. 59, no. 9, pp. 6018–6048, 2013.
- [2] Z. Babar, P. Botsinis, D. Alanis, S. X. Ng, and L. Hanzo, "Fifteen years of quantum LDPC coding and improved decoding strategies," *IEEE Access*, vol. 3, pp. 2492–2519, 2015.
- [3] J. X. Li and P. O. Vontobel, "LP decoding of quantum stabilizer codes," in *Proc. IEEE 2018 Int. Symp. Inf. Theory*, Vail, Colorado, USA, June 17–22 2018, pp. 1306–1310.
- [4] Y.-H. Liu and D. Poulin, "Neural belief-propagation decoders for quantum error-correcting codes," *arXiv preprint arXiv:1811.07835*, 2018.
- [5] J.-P. Tillich and G. Zémor, "Quantum LDPC codes with positive rate and minimum distance proportional to the square root of the blocklength," *IEEE Trans. Inf. Theory*, vol. 60, no. 2, pp. 1193–1202, 2014.
- [6] D. J. MacKay, G. Mitchison, and P. L. McFadden, "Sparse-graph codes for quantum error correction," *IEEE Trans. Inf. Theory*, vol. 50, no. 10, pp. 2315–2330, 2004.
- [7] M. A. Nielsen and I. L. Chuang, *Quantum Computation and Quantum Information*. UK: Cambridge University Press, 2010.
- [8] D. A. Lidar and T. A. Brun, *Quantum Error Correction*. Cambridge University Press, 2013.
- [9] J. X. Li and P. O. Vontobel, "Factor-graph representations of stabilizer quantum codes," in *Proc. 54th Allerton Conf. on Communication, Control, and Computing*, Allerton House, Monticello, IL, USA, Sep. 28–30 2016, pp. 1046–1053.
- [10] J. S. Yedidia, W. T. Freeman, and Y. Weiss, "Constructing free-energy approximations and generalized belief propagation algorithms," *IEEE Trans. Inf. Theory*, vol. 51, no. 7, pp. 2282–2312, Jul. 2005.
- [11] H. D. Pfister and P. O. Vontobel, "On the relevance of graph covers and zeta functions for the analysis of SPA decoding of cycle codes," in *Proc. IEEE 2013 Int. Symp. Inf. Theory*, Istanbul, Turkey, July 7–12 2013, pp. 3000–3004.
- [12] H. Wymeersch, F. Penna, and V. Savić, "Uniformly reweighted belief propagation: A factor graph approach," in *Proc. IEEE Int. Symp. Inf. Theory*, Saint-Petersburg, Russia, July, 31 – August, 5 2011, pp. 2000–2004.
- [13] D. Poulin and Y. Chung, "On the iterative decoding of sparse quantum codes," *Quantum Information and Computation*, vol. 8, no. 10, pp. 987–1000, 2008.
- [14] A. Hutter, J. R. Wootton, and D. Loss, "Efficient Markov chain Monte Carlo algorithm for the surface code," *Phys. Rev. A*, vol. 89, no. 2, p. 022326, 2014.